Stochastic multi-value cellular automata models for bicycle flow

2004 J. Phys. A: Math. Gen. 37 2063

(http://iopscience.iop.org/0305-4470/37/6/007)

INSTITUTE OF PHYSICS PUBLISHING JOURNAL OF PHYSICS A: MATHEMATICAL AND GENERAL

J. Phys. A: Math. Gen. **37** (2004) 2063–2072 PII: S0305-4470(04)68711-7

Stochastic multi-value cellular automata models for bicycle flow

Rui Jiang, Bin Jia and Qing-Song Wu

School of Engineering Science, University of Science and Technology of China, Hefei 230026, People's Republic of China

E-mail: qswu@ustc.edu.cn

Received 9 September 2003, in final form 28 November 2003
Published 28 January 2004
Online at stacks.iop.org/JPhysA/37/2063 (DOI: 10.1088/0305-4470/37/6/007)

Abstract

In this paper, the stochastic randomization is introduced in two different multi-value cellular automata (CA) models in order to model the bicycle flow. It is shown that with the randomization effect considered, the multiple states in the deterministic multi-value CA models disappear and the unique flow-density relations (fundamental diagrams) exist. The fundamental diagrams, the spacetime plots of the two models, are studied in detail. It is found that the transition from free flow to congested flow is smooth in one model while it is of second order in the other model. The comparison of the results of the two models indicates that in the bicycle flow, the priority of the movement should be given to slow bicycles in order to reach a larger maximum flow rate.

PACS numbers: 45.70.Vn, 05.70.Fh, 02.60.Cb

1. Introduction

In the past few decades, traffic problems have attracted the interest of many physicists [1–4]. Traffic flow is a kind of many-body system of strongly interacting cars and occurrence of traffic jams can be regarded as a kind of phase transition. To understand the behaviour of the traffic flow, various traffic-flow models have been proposed and studied, including car-following models, cellular automaton (CA) models, gas-kinetic models and hydrodynamic models [5–13]. Compared to other dynamical approaches, CA models are conceptually simpler, and can be easily implemented on computers for numerical investigations.

The rule-184 CA [14] has been widely used as a prototype for traffic flow. In 1992, Nagel and Schreckenberg proposed the well-known Nagel–Schreckenberg (NS) model [6]. As an extension of rule-184 CA, velocities $v_{\max} > 1$ are allowed in the NS model. The NS model can reproduce some basic phenomena encountered in real traffic. However, it cannot explain all experimental results. Therefore, several improved versions of the NS model were proposed, such as the slow-to-start (STS) models [7], etc. Nevertheless, these NS-based CA models

cannot describe real congested patterns at freeway bottlenecks. Based on the three-phase traffic theory, Kerner *et al* presented a new CA model, which can reproduce the real congested patterns (see e.g. [15] and references therein).

Recently, Nishinari and Takahashi [16, 17] have proposed a family of multi-value CA models. Different from previous ones, in these models, each site is assumed to hold L cars at most. The basis of the family is obtained from an ultradiscretization of the Burgers equation, so it is called Burgers cellular automaton (BCA). Its evolution equation is

$$U_j^{t+1} = U_j^t + \min\left(U_{j-1}^t, L - U_j^t\right) - \min\left(U_j^t, L - U_{j+1}^t\right) \tag{1}$$

where U_j^t represents the number of cars at site j and time t. If it is assumed that the road is an L-lane freeway, then the model can describe the multi-lane traffic without explicitly considering the lane-changing rule.

The maximum velocity of cars in BCA is 1, and Nishinari and Takahashi have extended BCA for the case of maximum velocity 2 [17] and presented two extended BCA (EBCA) models: EBCA1 and EBCA2. However, extension of BCA to general velocities is found to be difficult since the number of neighbouring sites becomes large [18]. In this sense, the BCA family is not appropriate for vehicle flow because the maximum velocities of vehicles are always quite large (generally taken as 5).

Nevertheless, we argue that the BCA family is suitable to describe the bicycle flow for the following reasons: (i) the maximum velocities of bicycles are relatively small (it can be taken as 2 (i.e., 14.4 km h^{-1}) if each site is assumed to be 2 m and one time step corresponds to 1 s)[1], (ii) bicycle lanes are not so distinctly partitioned as vehicle lanes, and the lane-changing behaviour of bicycles is much more complicated than that of vehicles; (iii) if one insists on modelling the lane-changing behaviour of bicycles explicitly, one will face very complex rules and calculations because the number of bicycle lanes is usually quite large.

For the above-mentioned reasons, the EBCA models are used to model the bicycle flow in this paper[2]. In the works of Nishinari and Takahashi, only the deterministic case is studied. In real traffic, bicycles are considered to be always perturbed by some traffic noises. Therefore, we introduce the stochastic randomization in EBCA1 and EBCA2 in this paper and study the randomization effect in the multi-value CA models.

This paper is organized as follows. In section 2, the EBCA1 and the EBCA2 are briefly reviewed and the stochastic randomization is introduced. In section 3, the simulation results are presented and analysed. The conclusions are given in section 4.

2. Stochastic multi-value models

In the EBCA models, a bicycle is assumed to be able to advance by two sites per time step. In the EBCA1 model, slow bicycles with speed 1 move prior to fast ones with speed 2. The bicycle movement from t to $t + 1$ consists of the following two successive procedures:

(a) bicycles move to their next site if the site is not fully occupied;
(b) only bicycles which moved in procedure (a) can move another one site if their next site is not fully occupied after procedure (a).

Therefore, the evolution equation of the EBCA1 is given by

$$U_j^{t+1} = U_j^t + b_{j-1}^t - b_j^t + c_{j-2}^t - c_{j-1}^t. \tag{2}$$

[1] The disorder effects may play an important role in bicycle flow. In this paper, the study is confined to homogeneous riders with maximum velocity 2. The bicycle flow of heterogeneous riders will be our future work.

[2] According to our daily experiences in China, there usually exist unidirectional bicycle lanes alongside vehicle lanes. Therefore, counterflow of bicycles rarely appears and it is not investigated here.

Here $b_j^t = \min\left(U_j^t, L - U_{j+1}^t\right)$ represents the number of moving bicycles at site j and time t in procedure (a); $c_j^t = \min\left(b_j^t, L - U_{j+2}^t - b_{j+1}^t + b_{j+2}^t\right)$ represents the number of moving bicycles that can move in procedure (b).

To introduce stochastic randomization, we suppose that the number of bicycles that can move two sites decreases by 1 with the probability p. Thus, the parallel update rules of stochastic EBCA1 are as follows:

1. calculation of b_j^t and c_j^t ($j = 1, 2, \ldots, K$, K is the number of sites);
2. randomization: $c_j^t = \max\left(c_j^t - 1, 0\right)$ with probability p;
3. update of U_j according to equation (2).

In contrast to EBCA1, fast bicycles with speed 2 move prior to slow ones with speed 1 in the EBCA2. Therefore, the evolution equation of the EBCA2 is given by

$$U_j^{t+1} = U_j^t + a_{j-2}^t - a_j^t + d_{j-1}^t - d_j^t. \tag{3}$$

Here $a_j^t = \min\left(U_j^t, L - U_{j+1}^t, L - U_{j+2}^t\right)$ represents the number of bicycles at site j that can move two sites forward; $d_j^t = \min\left(b_j^t - a_j^t, L - U_{j+1}^t - a_{j-1}^t\right)$ represents the number of bicycles that move only one site forward.

Similarly to EBCA1, the stochastic randomization is introduced by assuming that the number of bicycles that can move two sites decreases by 1 with the probability p. Thus, the parallel update rules of stochastic EBCA2 are as follows:

1. calculation of a_j^t, b_j^t and d_j^t ($j = 1, 2, \ldots, K$);
2. randomization: $a_j^t = \max\left(a_j^t - 1, 0\right)$ with probability p;
3. update of U_j according to equation (3).

3. Simulation results

In this section, the simulation results of stochastic EBCA1 and EBCA2 are presented and discussed. Firstly we study stochastic EBCA2.

3.1. Stochastic EBCA2

In figure 1, we show the fundamental diagrams of EBCA2. Note that the flow rate Q is defined by

$$Q^t = \frac{1}{KL}\sum_{j=1}^{K}\left(a_{j-2}^t + a_{j-1}^t + \mathrm{d}_{j-1}^t\right) \tag{4}$$

because a_{j-1}^t represents the number of bicycles that pass the site j.[3] The parameter values are $L = 4$, $K = 100$. The periodic boundary condition is applied. Figure 1(a) shows the fundamental diagram of deterministic EBCA2. One can see that multiple states exist around a critical density ρ_c, and this phenomenon has been explained in [17]. Note that in the fundamental diagram, the initial conditions are given by a finite random state, therefore, such highly ordered high flow states as ... 22222 ... are not reached.

Figure 1(b) shows the fundamental diagrams of stochastic EBCA2 of different p. One can see that with the stochastic randomization introduced, the multiple states disappear and the unique flow–density relation occurs instead. This means that the multiple states are not stable

[3] Note that a_{j-1}^t and a_{j-2}^t here as well as c_{j-2}^t in equation (5) are the actual numbers of bicycles that move two sites when the randomization is considered.

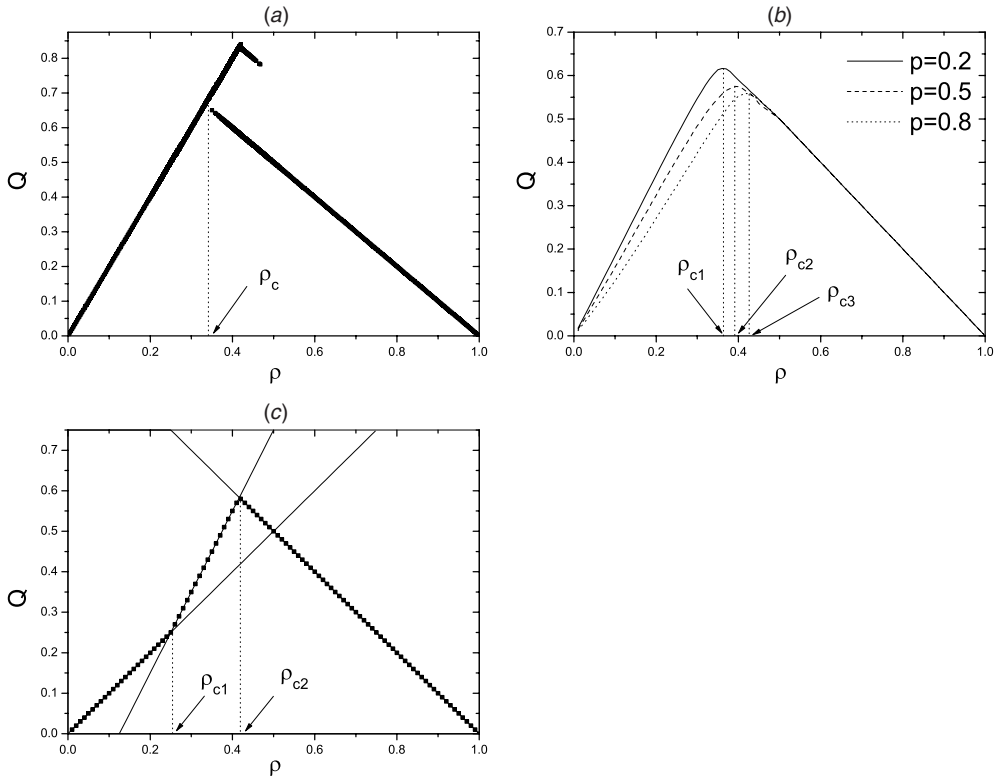

Figure 1. The fundamental diagram of EBCA2 . In (*a*) $p = 0$; (*b*) $p = 0.2, 0.5, 0.8$; (*c*) $p = 1$. In (*b*) ρ_{c1}, ρ_{c2} and ρ_{c3} denote the critical densities for $p = 0.2, 0.5, 0.8$, respectvely. In (*c*) the solid lines are the analytical result and the points are the simulation result.

with respect to the stochastic randmization. (One can compare the results with those of the velocity effect (VE) model [19]. In the deterministic VE model, the hysteresis phenomenon and metastable states exist, but they disappear when the randomization is introduced.) With the increase in p, the maximum flow decreases, the critical density ρ_c at which the maximum flow is reached increases. Moreover, we note that the transition from the free flow to congested flow is smooth in the stochastic EBCA2.

Next we investigate the spacetime structure of the stochastic EBCA2. To this end, we choose $p = 0.5$ for the representation. For this case, the critical density is approximately 0.393. Figure 2 shows the spacetime plots of the stochastic EBCA2 starting from random initial conditions. When the density is low, the bicycles are in free flow and the sites are seldom in the state $U = 4$ (not shown). However, when the density is near to the critical density, small jams begin to appear (shown by the arrows in figure 2(*a*)). We also note that the sites in the state $U = 4$ are not successive, which means that the jams are sparse[4].

When the density is a little larger than the critical density, the system is in a complex state: it transforms between the state of one large sparse jam (figure 2(*b*)) and the state of many small sparse jams (figure 2(*c*)). If one continues increasing the density, a compact jam appears in the sparse jam (figure 2(*d*)).

[4] A site is defined to be in a sparse jam if no bicycle in the site can move with velocity 2 and in a compact jam if no bicycle can move.

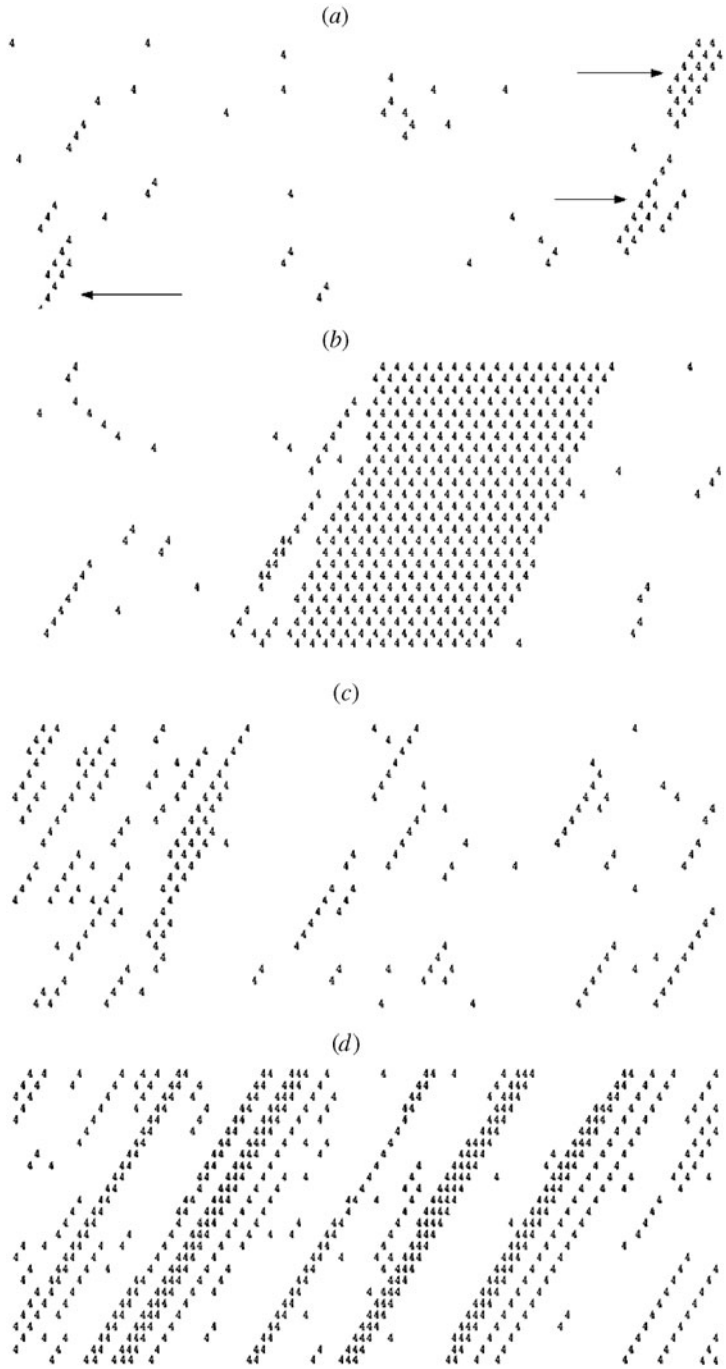

Figure 2. The spacetime plots of stochastic EBCA2. In (*a*) $\rho = 0.38$, (*b*), (*c*) $\rho = 0.4325$, (*d*) $\rho = 0.5325$. The bicycles move from left to right and the vertical direction (down) is (increasing) time. Here only the sites in the state $U = 4$ are shown. (*b*) and (*c*) start from the same initial condition and they display the system states at different time intervals.

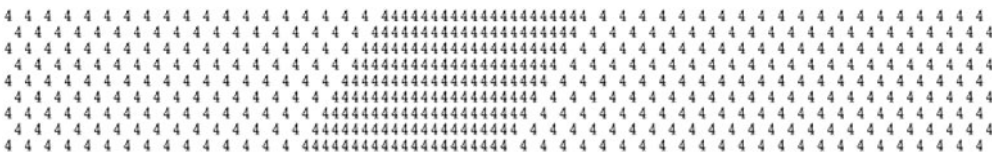

Figure 3. The spacetime plot of stochastic EBCA2 starting from a megajam. Here $\rho = 0.6$.

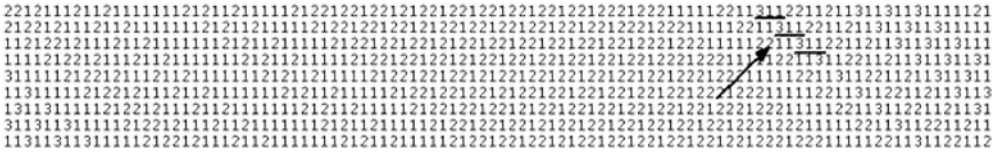

Figure 4. The spacetime plot of stochastic EBCA2. Here $\rho = 0.37$, $p = 1$.

Nevertheless, we should point out that different spacetime structures are obtained for density $\rho \geqslant 0.5$ if starting from a megajam, for example, see figure 3. In this case, the system is a coexistence of sparse jam and compact jam, and the stochastic randomization does not work because no bicycle can move with speed 2.

Finally, we focus on the special case $p = 1$. The fundamental diagram of $p = 1$ is shown in figure 1(c). Different from $0 < p < 1$, the fundamental diagram is composed of three straight lines. When $\rho < \rho_{c1}$, our simulations show that the maximum value of U_j is 1. Thus, every bicycle can move with speed 2 if the randomization is not considered. Obviously when the randomization is considered, the average speed of a bicycle is $2 - p$, so $Q = (2 - p) \times \rho$. When $\rho_{c1} < \rho < \rho_{c2}$, our simulations show that the maximum value of U_j is 3 and the minimum value of U_j is 1. Moreover, the value of U of the successive two sites preceding the site $U_j = 3$ is 1 (shown by the arrows in figure 4). Therefore, every bicycle can also move with speed 2 if the randomization is not considered. The average number of bicycles at site j is $\rho \times L$. As a result, the average speed of the bicycles at site j is calculated by $\frac{(\rho \times L-1)\times 2+1\times(2-p)}{\rho \times L} = 2 - \frac{p}{\rho \times L}$. So $Q = 2 \times \rho - p/L$. When $\rho > \rho_{c2}$, the average speed of the bicycles is determined by the vacancies. Thus, the average speed is calculated by $\frac{L\times K-L\times K\times \rho}{L\times K\times \rho} = 1/\rho - 1$. So $Q = (1 - \rho)$. The analytical result is also shown in figure 1(c), and it is in exact agreement with the simulations.

3.2. Stochastic EBCA1

In figure 5, we show the fundamental diagrams of EBCA1. Here the flow rate Q is defined by

$$Q^t = \frac{1}{KL} \sum_{j=1}^{K} \left(b_{j-1}^t + c_{j-2}^t \right). \tag{5}$$

The parameter value is still $L = 4$. The periodic boundary condition is applied.

Figure 4(a) shows the fundamental diagram of deterministic EBCA2. The multiple state effect is enhanced when compared with that of the EBCA2. Similarly, highly-ordered high-flow states are not reached in the fundamental diagram because of the finite random initial conditions.

Figure 4(b) shows the fundamental diagrams of stochastic EBCA1 of different p. As in EBCA2, with the stochastic randomization introduced, the multiple states disappear and the unique flow-density relation occurs. This point needs to be emphasized because in the deterministic EBCA1, there exist some states stable against a weak perturbation [17].

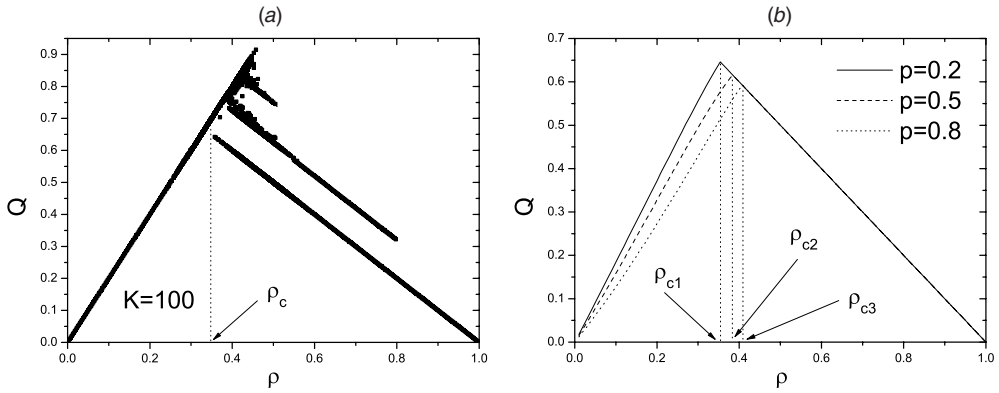

Figure 5. The fundamental diagram of the EBCA1. In (*a*) $p = 0$; (*b*) $p = 0.2, 0.5, 0.8$. In (*b*) $K = 5000$ is used because a small value of K leads to the finite size effect. We suppose the finite size effect correlates with the second-order phase transition (see the main text). In (*b*) ρ_{c1}, ρ_{c2} and ρ_{c3} denote the critical densities for $p = 0.2, 0.5, 0.8$, respectvely.

With the increase in p, the maximum flow decreases, the critical density ρ_c at which the maximum flow is reached increases. However, we note that the transition from free flow to congested flow is sharp in the stochastic EBCA1, it is a second-order phase transition. We can compare the phase transitions of stochastic EBCA2 and EBCA1 with that in the NS model. In the NS model with $p > 0$, the transition from free flow to congested flow is smooth (cf stochastic EBCA2). However, it is a second-order phase transition for the NS model when $p = 0$ because it is a sharp transition from the free flow branch to the congested flow branch (cf stochastic EBCA1). To our knowledge, it is the first stochastic CA model that shows a second-order phase transition from free flow to congested flow. The reason for this second-order phase transition will be investigated in our future work.

As in EBCA2, we investigate the spacetime structure of the stochastic EBCA1. We also choose $p = 0.5$ for representation. For this case, the critical density is approximately 0.383. Figure 5 shows the spacetime plots of the stochastic EBCA1. Similarly, when the density is low, the bicycles are in free flow and the sites are seldom in the state $U = 4$ (not shown). However, different from EBCA2, even when the density is near to the critical density, there is no jam although the sites in the state $U = 4$ appear (figure 6(*a*)). This may partly explain the existence of the second-order phase transition. When the density exceeds the critical density, a compact jam appears (figure 6(*b*)).

When starting from a megajam, the spacetime plots are somewhat different for large densities, for example, see figures 6(*c*), (*d*). One obtains a large compact jam from the megajam while many small compact jams from random initial conditions.

We also focus on the special case $p = 1$. The simulations show that the fundamental diagram of the EBCA1 is identical to that of the EBCA2. For $\rho < \rho_{c1}$, the maximum value of U_j is 1. When $\rho > \rho_{c2}$, the average speed of the bicycles is determined by the vacancies. These are similar to the EBCA2. However, in the density range $\rho_{c1} < \rho < \rho_{c2}$, although we still have the maximum value of U_j is 3 and the minimum value of U_j is 1, the value of U of the site $j + 2$ preceding the site $U_j = 3$ may be 2 (shown by the arrows in figure 7). But this can still guarantee that every bicycle moves with speed 2 if the randomization is not considered. Thus, the flow is still calculated as in EBCA2.

Finally, we compare the fundamental diagrams of stochastic EBCA1 and EBCA2 in figure 8. One can see that the maximum flow rate of the EBCA1 is larger than that of EBCA2.

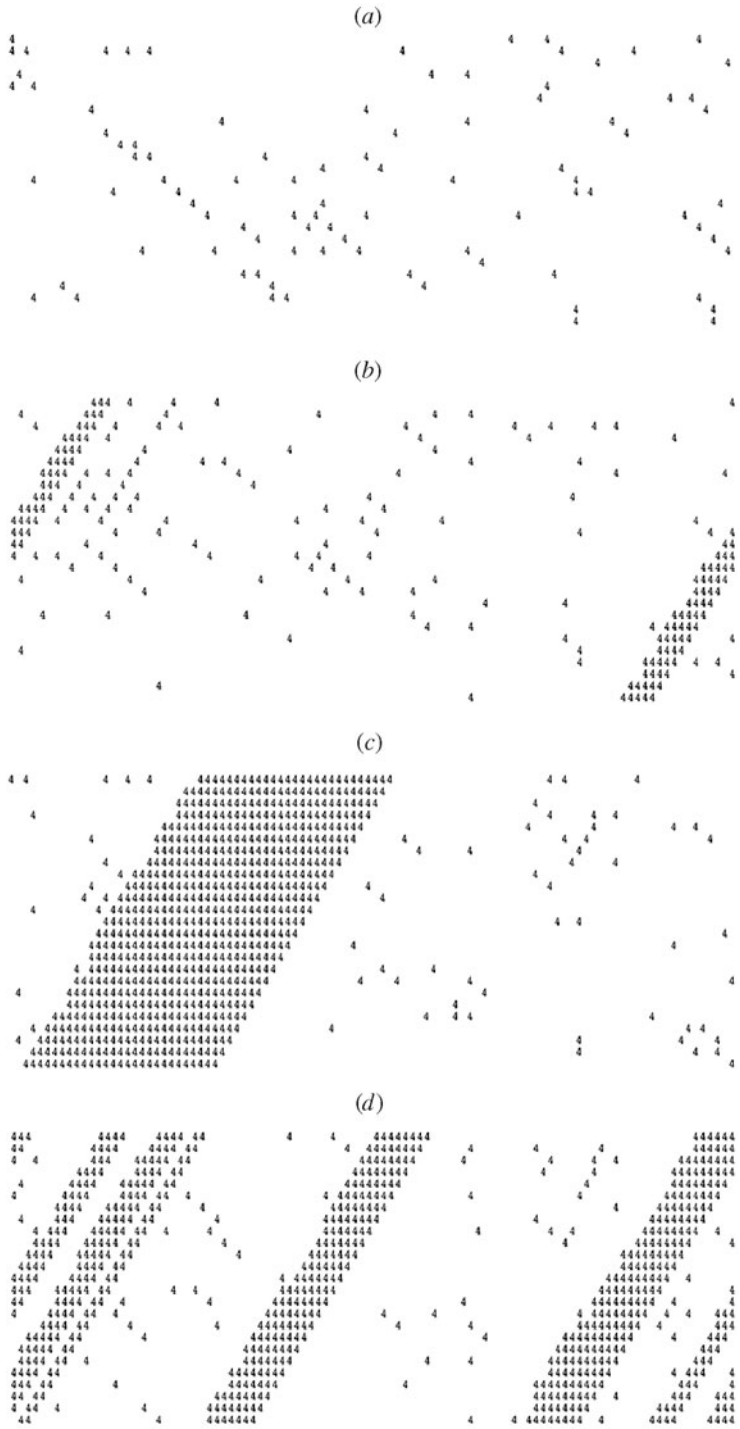

Figure 6. The spacetime plots of stochastic EBCA1. In (*a*) $\rho = 0.38$; (*b*) $\rho = 0.4125$; (*c*), (*d*) $\rho = 0.555$. Part (*c*) starts from a megajam and (*a*), (*b*), (*d*) start from random initial conditions.

Figure 7. The spacetime plot of stochastic EBCA1. Here $\rho = 0.38$, $p = 1$.

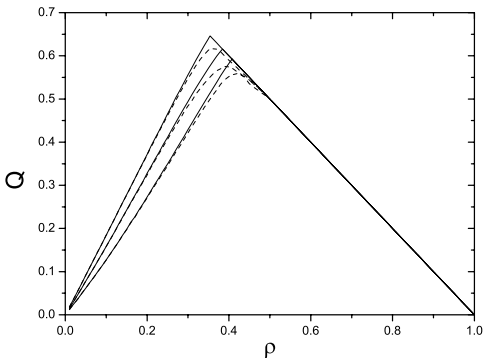

Figure 8. The comparison of stochastic EBCA1 (solid) and EBCA2 (dashed). From top to bottom, $p = 0.2, 0.5, 0.8$.

This enlightens us to suggest that in the bicycle flow, priority of movement should be given to slow bicycles in order to reach a larger maximum flow rate.

4. Conclusion

In this paper, the stochastic randomization effect in the two multi-value CA models: EBCA1 and EBCA2, has been investigated. We have demonstrated that the multi-value CA models are suitable to describe the bicycle flow.

The simulations show that with the randomization effect considered, the multiple states in the deterministic multi-value CA models disappear and unique flow–density relations occur. The fundamental diagrams, the spacetime plots of the two models, are studied in detail. It is found that the transition from free flow to congested flow is smooth in stochastic EBCA2 while it is second order in stochastic EBCA1. The special case of $p = 1$ in both stochastic EBCA2 and stochastic EBCA1 is studied. The analytical result is presented and it is in exact agreement with the simulation results. The comparison of the results of the two models indicates that in the bicycle flow, priority of movement should be given to slow bicycles in order to reach a larger maximum flow rate.

In our future work, the applicability of our results to real bicycle flow and the limitations need to be examined. In this context, it would be interesting to know whether, e.g., the jamming transition in the model has ever been observed empirically for bicycle flow. In fact, the observation of real bicycle flow is in preparation.

Acknowledgments

We acknowledge the support from the National Natural Science Foundation in China (NNSFC) with grant no 10272101 and the Youth Foundation of USTC with grant no KB1330.

References

[1] Schreckenberg M and Wolf D E (ed) 1998 *Traffic and Granular Flow '97* (Singapore: Springer)
Helbing D, Herrmann H J, Schreckenberg M and Wolf D E (ed) 2000 *Traffic and Granular Flow '99* (Berlin: Springer)
[2] Chowdhury D, Santen L and Schadschneider A 2000 *Phys. Rep.* **329** 199
[3] Helbing D 2001 *Rev. Mod. Phys.* **73** 1067
[4] Nagatani T 2002 *Rep. Prog. Phys.* **65** 1331
[5] Bando M *et al* 1995 *Phys. Rev.* E **51** 1035
Helbing D and Tilch B 1998 *Phys. Rev.* **58** 133
Jiang R, Wu Q S and Zhu Z J 2001 *Phys. Rev.* **64** 017101
Treiber M, Hennecke A and Helbing D 2000 *Phys. Rev.* **62** 1805
Tomer E, Safonov L and Havlin S 2000 *Phys. Rev. Lett.* **84** 382
[6] Nagel K and Schreckenberg M 1992 *J. Physique* I **2** 2221
[7] Benjamin SC S C, Johnson N F and Hui P M 1996 *J. Phys. A: Math. Gen.* **29** 3119
Barlovic R, Santen L and Schadschneider A *et al* 1998 *Eur. Phys. J.* B **5** 793
[8] Helbing D *et al* 2001 *Transp. Res.* B **35** 183
[9] Lighthill M J and Whitham G B 1995 *Proc. R. Soc.* A **229** 317
[10] Payne H J 1971 *Mathematical Models of Public Systems* vol 1 ed G A Bekey (La Jolla, CA: Simulation Council)
[11] AW A and Rascle M 2000 *SIAM J. Appl. Math.* **60** 916
[12] Jiang R, Wu Q S and Zhu Z J 2001 *Chin. Sci. Bull.* **46** 345
Jiang R, Wu Q S and Zhu Z J 2002 *Transp. Res.* B **36** 405
[13] Lee H Y, Lee H W and Kim D 1998 *Phys. Rev. Lett.* **81** 1130
Lee H Y, Lee H W and Kim D 1999 *Phys. Rev.* E **59** 5101
[14] Wolfram S 1986 *Theory and Applications of Cellular Automata* (Singapore: World Scientific)
[15] Kerner B S *et al* 2002 *J. Phys. A: Math. Gen.* **35** 9971
[16] Nishinari K and Takahashi D 1998 *J. Phys. A: Math. Gen.* **31** 5439
[17] Nishinari K and Takahashi D 1999 *J. Phys. A: Math. Gen.* **32** 93
Nishinari K and Takahashi D 2000 *J. Phys. A: Math. Gen.* **33** 7709
[18] Nishinari K 2001 *J. Phys. A: Math. Gen.* **34** 10727
[19] Li X B *et al* 2001 *Phys. Rev.* E **64** 066128